PERFORMANCE ANALYSIS ON OPERATION OF DAYTIME GRATING SELECTIVE PASSIVE SKY RADIATIVE COOLING SYSTEM IN BUILDING

by

Zhijian ZHANG[a*], Liang WANG[b], Fenghao SHI[a], and Sukun CHEN[a]

[a] Sichuan Institute of Building Research, Chengdu, Sichuan, China
[b] Southwest University of Science and Technology, Mianyang, Sichuan, China

Original scientific paper
https://doi.org/10.2298/TSCI240722079Z

Passive sky radiative cooling technology has attracted recent interest due to achieve sub-ambient cooling with the advantages of not consuming additional energy and not producing pollutants. However, the practical utility of sky radiative cooling technology in building applications remains under-explored, which requires not only the rational design and integration of the system, but also different control strategies. A novel grating selective passive sky radiative cooling (GS-PSRC) system for building cooling was constructed and five control strategies were used to simulate and analyses the operation of a 50 m^2 office building located in Chengdu area during the hottest week of summer in this work. The study shown that the system is able to maintain the average indoor temperature around 20 °C during the hottest period and achieve a temperature difference ranging from 3.39-10.77 °C, which provides a good cooling capacity. But the excessive outdoor wind speed inhibits the cooling capacity of the GS-PSRC system, which leads to the lower average COP of the system in summer. Its application was further studied across various climate zones. Results indicated the cooling performance of the system mainly be affected by wind speed in different climate zones. Adding wind-blocking devices around radiators is recommended to improve cooling efficiency. This work fully demonstrates the potential application of passive sky radiative cooling technology in building energy efficiency.

Key words: *grating selective structure, building energy consumption, radiative cooling*

Introduction

Global warming, population growth, industrial development, and rising living standards in emerging and developing economies have led to a dramatic increase in energy demand for refrigeration and air conditioning worldwide. It is estimated that cooling has consumed 15% of global electricity and generated 10% of GHG emissions [1-3]. Furthermore, the cooling demand is expected to increase tenfold by 2050 and direct emissions from conventional cooling technologies will reach 45% of CO_2 emissions by 2050 [4]. Therefore, the development of energy-saving and eco-friendly cooling technologies is essential to avoid these issues and achieve a sustained low carbon lifestyle. However, emerging forms of renewable energy-driven cooling still require rather complex integrated systems to convert renewable energy into other forms of energy such as electricity, which can subsequently be utilized for cooling when possible. In

* Corresponding author, e-mail: Zhangzj1220@163.com

addition, integrated systems such as solar, hydro and wind powered electric cooling have low conversion efficiencies, occupy a large area and are limited by time and geography [5-7]. The development of novel cooling systems that can be simple to integrated with a wide range of applications is essential in order to achieve a sustainable low carbon paradigm.

Compared with the aforementioned cooling methods, passive sky radiative cooling technology has greatly aroused the interest of many scholars with the advantages of not consuming additional energy and not producing pollutants in recent years [8-14]. The passive sky radiative cooling technology mainly relies on the absorption of solar radiation and atmospheric radiation on the surface of the radiator, and uses the atmospheric window (8-13 μm) to emit its own heat directly into the outer space, where the radiant heat is exchanged with the space, thus realizing its own passive cooling [15-19]. It has great potential in solving the problems of energy consumption and global warming effect caused by the current vapor compression-dominated cooling technology.

In general, the development of daytime radiative cooling is of greater research interest than the nighttime radiative cooling first reported in the 1970's [20], since peak cooling loads usually occur during the daytime. This requires that the radiator surface under direct sunlight during the daytime has both a high emissivity in the atmospheric window band and a high reflectivity in the solar band to produce effective cooling. Due to the difficulty in achieving this property, it was not until 2014 that the feasibility of daytime radiative cooling was first demonstrated experimentally by a radiator consisting of a multilayer material [8]. The publication of this work also officially opened the door to daytime radiative cooling, which has seen significant advances in the last few years in research on daytime radiative cooling in metamaterials [10, 21], porous materials [11, 22-24], grating structures [25-28], and nanomaterials [29-31]. All of these radiators were able to achieve a radiative cooling power of 50-100 W/m^2 under direct sunlight during the daytime, producing a good cooling effect.

Despite advances in materials and construction of radiators, the practical application of daytime radiative cooling in building thermal management still faces significant challenges at the system level. A number of issues, including system configuration and control, the impact of weather conditions, system cost and feedback cycles, need to be considered when designing a sky radiative cooling system. During the development of daytime radiative cooling systems, numerous scholars have attempted to use radiators to generate cold water at conditions lower than the ambient temperature during the daytime, which provides the advantage of higher cooling power regulation and greater efficiency gains for radiative cooling systems [15, 32-37]. Jeong *et al.* [38] integrated the radiators as a pre-cooler with a conventional HVAC system, which the cooling performance and indoor air temperature of the integrated system was carried out. It is showed that the system can significantly reduce the total energy consumption of the traditional air conditioning system when pre-cooling the ambient hot air, and can reduce the indoor air temperature by 10 °C. Zhang *et al*. [39] built a new hybrid radiative cooling system for single-family residential cooling in the USA region, and the results showed that the hybrid system can save 26%-46% of the air conditioning energy consumption per year. Wang *et al*. [40] also studied the energy saving potential of a photon emitter hybrid cooling system, stating that the photon emitting system can save 45%-68% of electrical energy compared to a VAV system as well as comparing it to the best available coated nighttime radiative cooling system. However, Wang *et al*. [40] did not compare the system with other daytime radiative cooling systems and therefore, lacks some conviction. Additionally, sky radiative cooling systems are usually combined with other cooling systems such as thermoelectric cooling systems [41, 42] as a supplemental cooling source for efficiency improvement to increase the COP of the system to

enhance indoor cooling. However, such composite systems are usually designed to be complex and costly with low economic benefits. Meanwhile, it is known in the research process that the performance of the sky radiative cooling system is easily affected by weather and environmental conditions, especially the outdoor temperature and wind speed changes, and the actual outdoor wind speed changes have not been considered in many researches but assumed to vary in a certain range, which makes it difficult to use the sky radiative cooling system directly for practical applications without control and operation strategies.

Herein, a simple and economic GS-PSRC system is constructed to better apply the sky radiative cooling technology in buildings in the study. Taking the Chengdu area as an example, five operation strategies are proposed considering the actual change of outdoor wind speed, and it is found that the outdoor wind speed is negatively correlated with the change of cooling capacity, but the cooling capacity produced by this system can still meet the demand of indoor cooling during the daytime and achieve the cooling effect of maintaining the indoor/outdoor temperature difference between 3~1 °C in the hottest week. Meanwhile, the operational performance of the system in different regions was studied, and the results showed that the cooling performance of the system in different climatic zones did not differ much, and had a strong adaptability.

System description

Grating selective passive sky radiative cooling system model

Figure 1 shows a schematic of the proposed GS-PSRC system. The system consists of a sky radiative cooling subsystem, a cold storage tank, a control subsystem and terminal device. The sky radiative cooling subsystem has multiple panels with the grating selective structure to provide 24 hours continuous cooling of fluid, and the secondary refrigerants used in the system is water. The control subsystem includes six thermocouples, four on/off controlled valves, and two on/off control pumps to automatically control the switching between five different operating modes. The indoor terminal unit is a fan coil system. In building integration, the sky radiative cooling subsystem is placed on a flat or low slope building roofs so that there is a large view factor from the radiators to the sky.

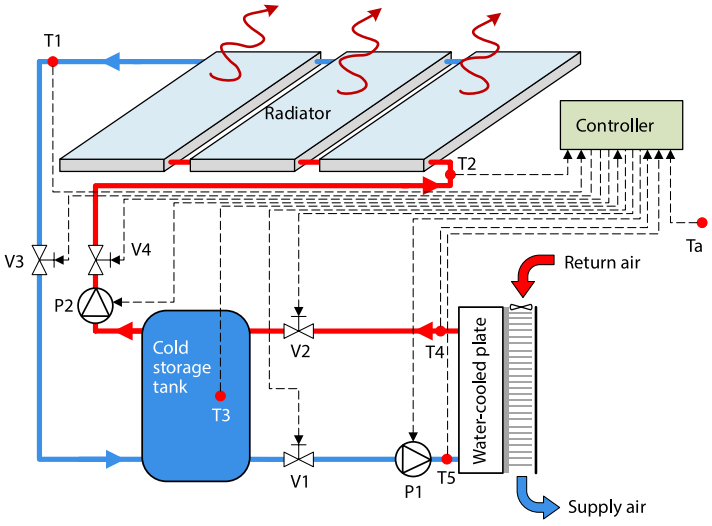

Figure 1. Schematic of GS-PSRC system

Building model

Chengdu city is selected as the calculation site in the study, and the simulated building is an office with a length of 10 m, a width of 5 m and a height of 3.5 m. The simulation process is only for the summer indoor cooling situation, the number of indoor air change is taken as one hourly. The building enclosure parameters, indoor occupants, mechanical equipment loads, and building occupancy times are shown in tabs. 1 and 2. It can be seen from fig. 2(a) that the annual temperature change curve of Chengdu, the highest temperature of the year is mainly concentrated in July, so the simulation time in this chapter is selected as the simulation time of one week in July to simulate the indoor temperature change. At the same time, according to heat gain of indoor personnel, lighting, equipment and the enclosure to calculate the indoor time-by-time cooling load, the results are shown in fig. 2(b).

Table 1. Parameters of building envelope

Enclosure parameters	Wall	Floor	Roof	Window
Heat transfer coefficient [$Wm^{-2}K^{-1}$]	0.8	0.5	0.5	3.2

Table 2. Indoor personnel, mechanical equipment loads and operating hours

Number of indoor persons	Power density of equipment	Load density of lighting	Air change rate	Operation time
6	11 W/m^2	18 W/m^2	1 time per hour	8:00-18:00

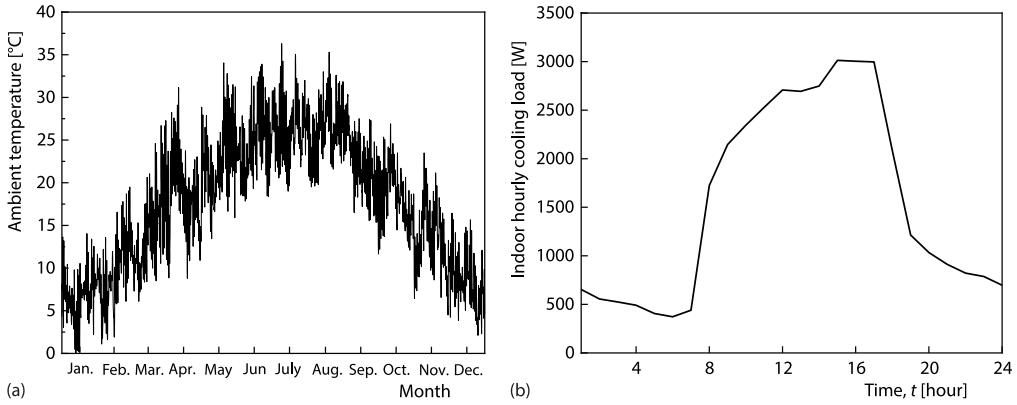

Figure 2. Temperature change and indoor load curve of Chengdu throughout the year; (a) annual temperature change curve and (b) indoor load curves

Modelling of the sky radiative cooling subsystem

The sky radiative cooling subsystem is mainly used to generate a certain amount of cold in the sub-ambient to exchange heat with the secondary refrigerants, the sub-system consists of grating selective radiators, the coolant channel, thermal insulation film, the schematic diagram is shown in fig. 3(a). The sky radiative cooling subsystem consists mainly of grating selective structure radiators with water flow channels connected to the lower side, the thickness of the connection is ignored in the calculation process. Thermal insulation devices are provided around the radiator and at the bottom of the channels to reduce heat transfer losses. The P_{rad} is the infrared thermal radiative power density on the radiator within the atmospheric window, P_{solar}

is the absorbed solar irradiation power density on the radiator, P_{atm} is the atmospheric radiative power absorbed by the radiator, and P_{non} radiative is the convective and conductive heat fluxes between the emitter and the ambient air. The grating selective radiator composed of a two-layer grating structure, whose material composition and structural dimensions are obtained by optimized solution [28], as shown in fig. 3(b). The structural parameters and radiative properties are taken from [28]. The emitter has an average reflectivity of 95.1% in the solar band and an average emissivity of 88.04% in the atmospheric window band. The bottom of the radiator is in direct contact with the refrigerant channel to cool the refrigerant below ambient temperature. It is assumed that the thermal resistance to heat transfer between the radiator and the refrigerant is negligible in the calculations. In addition, identical radiator panels can be connected in series/parallel for greater cooling capacity. Thermal insulation is provided around the radiators and at the bottom of the channels to minimize parasitic heat gain from the surrounding environment.

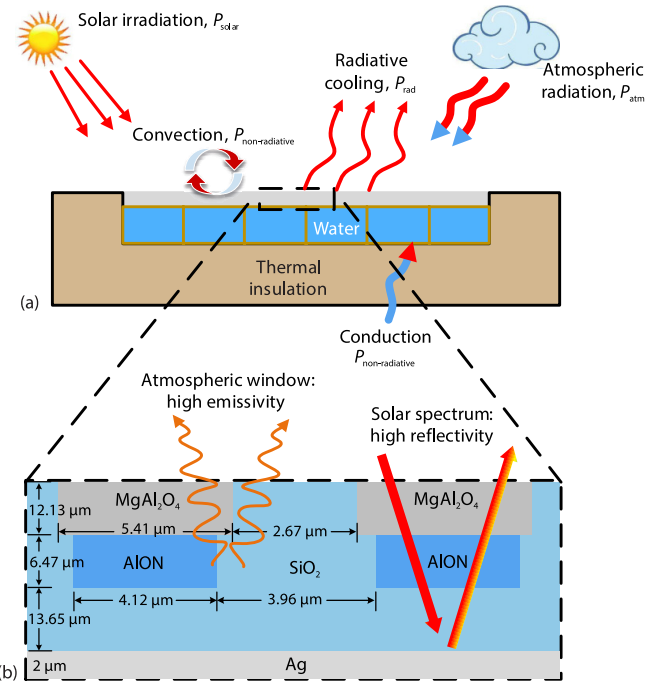

Figure 3. The sky radiative cooling subsystem and grating selective structure radiator; (a) schematic of the heat transfer process of the sky radiative cooling subsystem under the sun and (b) schematic of the grating selective structure radiator

According to conservation of energy, the net cooling power of the sky radiative cooling subsystem can be defined [43]:

$$P_{net} = P_{rad}(T_{rad}) - P_{solar} - P_{atm}(T_{atm}) - P_{non\text{-}radiative}(T, T_{amb}) \quad (1)$$

where P_{net} is the net cooling power generated by the sky radiative cooling subsystem, $P_{net} > 0$ means that the radiator can produce cold and *vs.*, $P_{rad}(T_{rad})$ – the infrared thermal radiative power on the radiator within the atmospheric window, T_{solar} – the total solar irradiation absorbed by the radiator, $P_{atm}(T_{atm})$ – the atmospheric radiative power absorbed by the radiator, and $P_{non\text{-}radiative}(T, T_{amb})$ – the convective and conductive heat fluxes between the emitter and the ambient air.

The emitted power $P_{rad}(T_{rad})$ generated by the radiator itself [8]:

$$P_{\text{rad}}(T_{\text{rad}}) = A\int \mathrm{d}\Omega \cos\theta \int_0^{\infty} \mathrm{d}\lambda I_B(T_{\text{rad}}, \lambda)\varepsilon_{\text{rad}(8\sim13)}(\lambda, \theta) \tag{2}$$

where $\varepsilon_{\text{rad}(8\sim13)}(\lambda, \theta)$ is the spectral angular emissivity and Ω – an integral over the hemispherical solid angle, it is expressed [8]:

$$\int \mathrm{d}\Omega = \int_0^{\pi/2} \mathrm{d}\theta \sin\theta \int_0^{2\pi} \mathrm{d}\varphi \tag{3}$$

where $I_B(T_{\text{rad}}, \lambda)$ is the intensity of a blackbody at temperature T_{rad}, it is expressed [8]:

$$I_B(T_{\text{rad}}, \lambda) = \frac{2hc^2}{\lambda^5} \frac{1}{\exp\left(\dfrac{hc}{\lambda k_B T_{\text{rad}}}\right) - 1} \tag{4}$$

where k_B is the Boltzmann's constant, h – the Planck's constant, c – the speed of light, and λ – the accounts for the wavelength.

The power P_{solar} absorbed from the sun is expressed [8]:

$$P_{\text{Sun}} = A\int_0^{\infty} \mathrm{d}\lambda \varepsilon_{\text{Sun}(0.3\sim4)}(\lambda, \theta_{\text{Sun}}) I_{AM1.5}(\lambda) \tag{5}$$

where $I_{AM1.5}(\lambda)$ is the solar spectral irradiation intensity of $AM1.5$.

By replacing the absorptivity of the selective radiator with its emissivity base on Kirchhoff's law, the absorbed power density $P_{\text{atm}}(T_{\text{atm}})$ from the atmosphere is given [8]:

$$P_{\text{atm}}(T_{\text{atm}}) = A\int \mathrm{d}\Omega \cos\theta \int_0^{\infty} \mathrm{d}\lambda I_B(T_{\text{atm}}, \lambda)\varepsilon_{\text{rad}(4\sim8)}(\lambda, \theta)\varepsilon_{\text{atm}}(\lambda, \theta) \tag{6}$$

where $\varepsilon_{\text{atm}}(\lambda, \theta) = 1 - t(\lambda)^{1/\cos\theta}$ is the spectral angular emittance of the atmosphere [44], which is closely related to factor such as atmospheric water content, aerosol conditions, and cloud cover. where $t(\lambda)$ is the atmospheric transmittance in the zenith direction [45].

Non-radiative heat power, $P_{\text{non-radiative}}$, generally consists of heat power generated by convection and conduction. Can be expressed:

$$P_{\text{non-radiative}}(T, T_{\text{amb}}) = Ah_{\text{cond+conv}}(T_{\text{amb}} - T) \tag{7}$$

where $h_{\text{cond+conv}}$ is the combined heat transfer coefficient. Due to the small thickness of the radiator, thermal conduction is not considered, and only the convective thermal power between the air and the emitter is considered.

Since the outdoor wind speed is transient, Reynolds number is introduced to represent the effect of different wind speeds on the heat transfer coefficient. Therefore, the convective heat transfer coefficient can be expressed:

– Fluid out-swept flat plate laminar heat transfer coefficient [46]

$$\frac{h_c l}{\lambda_{\text{air}}} = 0.664\,\text{Re}^{1/2}\,\text{Pr}^{1/3} \tag{8}$$

– Fluid out-swept flat plate turbulent heat transfer coefficient [46]:

$$\frac{h_c l}{\lambda_{\text{air}}} = (0.037\,\text{Re}^{4/5} - 871)\,\text{Pr}^{1/3} \tag{9}$$

where h_c is the convective heat coefficient and l, λ_{air} are the characteristic length and the thermal conductivity of air at ambient temperature, respectively.

In this study, the simulation of outdoor wind speed is achieved using the meteorological module built-in in the simulation software, obtaining local hourly wind speeds by importing hourly TMY2 weather data from different regions.

Verification of the sky radiative cooling power calculation model

According to radiative properties are taken from [28], the radiative cooling power calculation model is verified. The comparison of the calculation results with those in [47] is shown in the fig. 4. As can be seen from the figure, the calculated results of the radiative cooling power calculation model agree well with the literature results, verifying the reliability of the radiative cooling power calculation model.

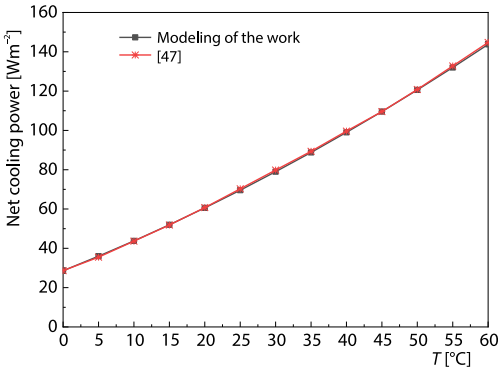

Figure 4. Comparison of the calculation results from this study and [47] to verify the validity of radiative cooling power calculation model

Control strategy of the control subsystem

In order to better apply the GS-PSRC system in the building, five working modes will be set up during the operation of the system, and detail of the control schemes are presented in tab. 3.

Table 3. Operational modes and control schemes of the GS-PSRC system

Working mode	Building cooling load	Brief description	Control method
1	No	$P_{net} < 0$, the radiator shutdown, stopping cold storage in the cold storage tank	P1-P2 off, V1-V4 off
2	No	$P_{net} > 0$, the radiator stores cooling energy in the cold storage tank	P1 off, P2 on, V3-V4 on, V1-V2 off
3	Yes	$P_{net} > 0$, the radiative cooling-cold storage series cooling mode is turned on cooling the room when the water temperature of the cold storage tank is higher than the threshold	P1 on, P2 on, V1-V4 on
4	Yes	$P_{net} > 0$, the radiator stops storing cold and the cold storage tank cools the room alone when the temperature of the cold storage tank is lower than the threshold value	P1 on, P2 off, V1-V2 on, V3-V4 off
5	Yes	$P_{net} < 0$, the radiator shutdown, the cold storage cools the room alone	P1 on, P2 off, V1-V2 on, V3-V4 off

The five control strategies are:

- Night shutdown mode: when the radiator is unable to produce cold, it stops storing cold to the cold storage tank.
- Cold storage mode: it stores cooling energy in the cold storage tank when there is no cold load in the room.
- Series cooling mode: the radiative cooling-cold storage series cooling mode is turned on when the water temperature of the cold storage tank is higher than the threshold.
- The cold storage tank separate cooling Mode 1: the radiator stops storing cold to it when the temperature of the cold storage tank is lower than the threshold value, and the cold storage tank individual cooling mode is turned on.

– The cold storage tank separate cooling Mode 2: the radiator stops storing cold to the cold storage tank when the radiator fails to produce cold, the cold storage tank individual cooling mode is turned on.

Initial parameter of the system

A few parameters need to be sized before conduction system simulation:

– The surface area of the GS-PSRC subsystem.
– The volume of the cold storage tank.
– The air volume of fan coil.
– The water supply of pump.

These parameters are initially sized according to the cooling load of the building.

The total radiative cooling surface area can be estimated based on indoor hourly cooling load. As shown in fig. 2(b), it can be seen that the maximum indoor cooling load is 3.013 kW. Therefore, the surface area of the radiator panels can be calculated to satisfy the maximum daytime cooling demand:

$$A_R = \frac{q_{\text{max\_cooling\_load}}}{\overline{q}_{\text{net}}} \tag{10}$$

where $q_{\text{max\_cooling\_load}}$ is the maximum indoor cooling load and $\overline{q}_{\text{net}}$ – the daily average net cooling power of the radiator, the net cooling power is 72.42 W/m^2 [29]. The surface area of the radiator was calculated to be 41.6 m^2.

The volume of cold storage tank can be sized:

$$V_{\text{tank}} = \frac{\sum_{j=1}^{24} \max[(q_{cooling\_\text{load},j} - \overline{q}_{\text{net}}), 0] \times 3600}{\rho_{\text{w}} c_{p,\text{w}} \Delta \overline{T}} \tag{11}$$

where $q_{\text{max\_cooling\_load},j}$ is the cooling load of the building in hour j ($1 \leq j \leq 24$), ρ_{w}, $c_{p,\text{w}}$, and ΔT are the density of water, the specific heat of water, and the average daily cold storage tank temperature difference, respectively. The ΔT is equal to 4 °C in the study. The volume of the cold storage tank is calculated to be 6 m^3 based on the indoor cold load and the average cooling capacity of the radiator in fig. 2(b).

The air volume of fan coil is calculated:

$$M = \frac{q_{\text{max\_cooling\_load}}}{c_{p,\text{air}} \Delta T_{\text{s,air}}} \tag{12}$$

where $c_{p,\text{air}}$ is the specific heat of air, take 1.005 kJ/kgK and $\Delta T_{\text{s,air}}$ – the design air supply temperature difference and take 8 °C. Through the eq. (12) can be calculated that the air supply volume is 1284 m^3 per hour.

The water supply from Pumps 1 and 2 is calculated:

$$L = \frac{q_{\text{max\_cooling\_load}}}{c_{p,w} \Delta T_{\text{s,w}}} \tag{13}$$

where $\Delta T_{\text{s,air}}$ is the supply and return water heat transfer temperature difference, take 5 °C. According to the eq. (13) can be calculated for the water supply 0.64 m^3 per hour.

The GS-PSRC system COP is calculated:

$$\text{COP} = \frac{Q_{net\_radiator}}{W_{system}} \tag{14}$$

where $Q_{net\_radiator}$ is the net cold generated by the radiator and W_{system} – the system power consumption.

Additionally, tab. 4 shows the device parameters of the GS-PSRC system. The initial conditions of the GS-PSRC system are determined, and the cooling simulation of the building is carried out to analyze its operational energy consumption and cooling COP.

Table 4. Device parameters of the GS-PSRC system

Type	Device number	Number	Value	Unit
Radiator area	–	1	42	[m^2]
Cold storage tank	–	1	6.28	[m^3]
Fan coiler	YGFC-14CC2ZXFXCLD	1	0.209	[kW]
Supply water pump	Wilo-NL 32/200-0.75/4	1	0.75	[kW]
Return water pump	Wilo-NL 32/200-0.75/4	1	0.75	[kW]
On/off controlling	–	2	0.06	[kW]

Results and discussion

System operation on typical summer

From to the hourly temperature change curve of Chengdu throughout the year, the hottest week of July is selected for simulation, and the main design parameters of the system are: the volume of the cold storage tank is 6.28 m^3, and the surface area of the radiators is 42 m^2. Figure 5 shows the operation of the GS-PSRC system and the change of indoor temperatures from July 7-13, and the daily maximum solar irradiations are between 520-973 W/m^2, and the daily maximum ambient temperatures are between 30.25 ℃ and 36.3 ℃ on these days. As can be seen in fig. 5(a), the average indoor temperature during the daily working hours showed an increasing trend, which was due to the lack of indoor cooling supply during the night, resulting in a gradual increase in the indoor temperature each night, but the average indoor temperature was much lower than the outdoor temperature during the working hours. In order to explore the maximum potential of GS-PSRC system in building refrigeration application, the indoor air supply was not changed during the study process, and the maximum air supply was used. The average indoor temperature during daily working hours is between 19.18 ℃ and 20.98 °C, which is lower than the outdoor temperature by an average of 3.39-10.77 °C. The temperature changes in the indoor and outdoor cover the human comfort temperature range, indicating that by applying this system and using variable frequency control technology. It is possible to realistically maintain indoor temperatures within the human comfort range. This shows that the GS-PSRC system has favorable cooling benefit in the building.

During the night period, it is shown from fig. 5(b) that the system mainly operates at Mode 2, and occasionally at Mode 1, which means that the sky radiators may stop supplying cold to the cold storage tanks during the night period, *i.e.*, when the cooling capacity is less than 0, the system is unable to produce cold by default, and therefore, the controller will stop running Pump 2 to storage cold. Meanwhile, through the temperature change curve of the cold storage tank, it can be seen that the temperature of the cold storage tank is rising every day when the daytime working time, and it can be learnt that the radiator almost does not supply cold to the cold storage tank. The temperature threshold of the cold storage tank is set to 7 ℃ in the calculation process, *i.e.*, when the temperature of the cold storage tank is higher than 7 ℃, the radiator should supply cold to the cold storage tank to maintain the temperature of the cold storage tank at 7 ℃ and below, but it can be found in fig. 5(b) that when the temperature of

the cold storage tank exceeds the temperature threshold, the system is almost not switched to Mode 4 for supplying cold to the cold storage tank but switched to Mode 5, which indicates that the radiator almost does not supply cold to the cold storage tank when daytime working hours. This indicates that the radiators are almost unable to produce cold when daytime working hours.

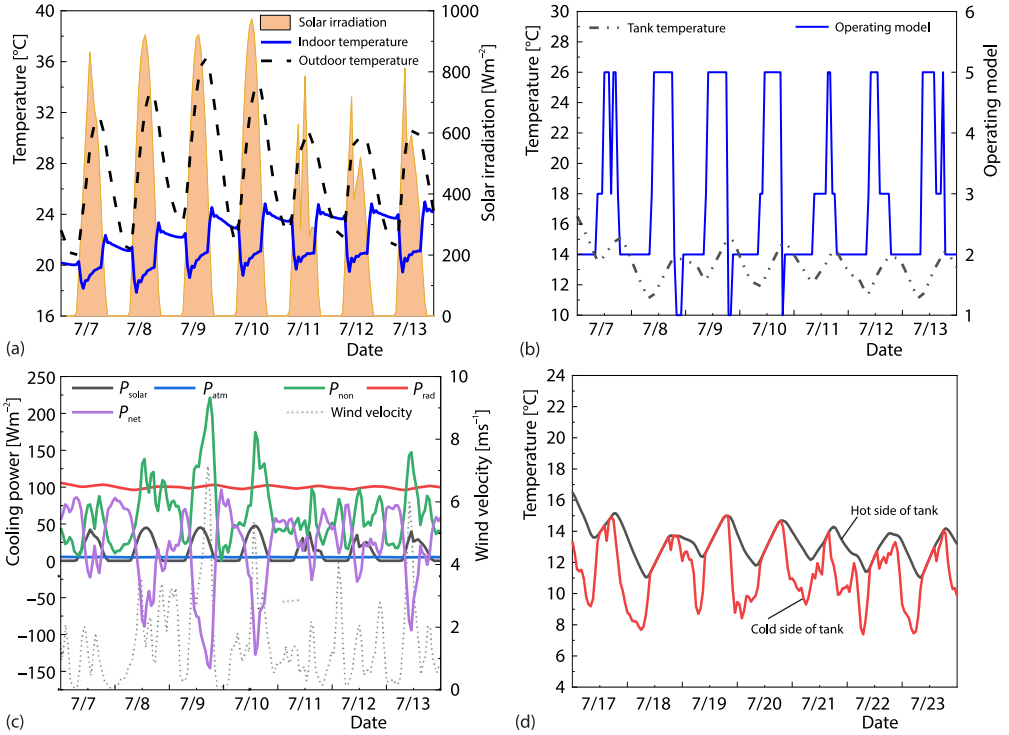

Figure 5. Performance of the GS-PSRC system on summer (July 7-13)

The reason why the radiators stopped supplying cooling to the cold storage can be learnt from fig. 5(c), that too much outdoor wind speed can lead to an increase in convective heat transfer and inhibit the radiators from generating cooling capacity, thus preventing the start-up of the GS-PSRC system. This shows that the cooling capacity produced by the radiators is negatively correlated with the outdoor wind speed, and excessive outdoor wind speed deteriorates the operational performance of the GS-PSRC system. Therefore, when the outdoor wind speed is too high throughout the year, it is not recommended to use the sky radiative cooling system to cool the room alone, or the dominant role of convective heat transfer can be weakened by adding wind-blocking devices around the radiators. Furthermore, it can be found from fig. 5(d) that due to the cooling effect of the radiators, the daily temperature difference of the cold storage tank can be maintained between 3.25 °C and 5.47 °C, and the average temperature of the cold storage tank does not exceed a maximum of 14 °C during the daytime working period, which also shows that the sky radiative cooling technology has a great potential to be applied to the energy saving of buildings.

Monthly system performance

Figure 6 illustrates the variation of the monthly average hourly cooling capacity and power consumption and COP between May and August. It can be concluded that the radiative

cooling capacity and consumed power are almost stable between May and August, as shown in fig. 6(a). The consumed power of the system includes power of pumps and fans. Since the room temperature threshold was not set in order to get the maximum cooling of the room during the calculation process, the Pump 1 and the fan were in operation all the time during the daytime working hours. This results in high actual monthly consumed power of the system, which makes the monthly COP of the system low. The average COP from May to August is 1.34, and the maximum COP of the system is 1.37 in July.

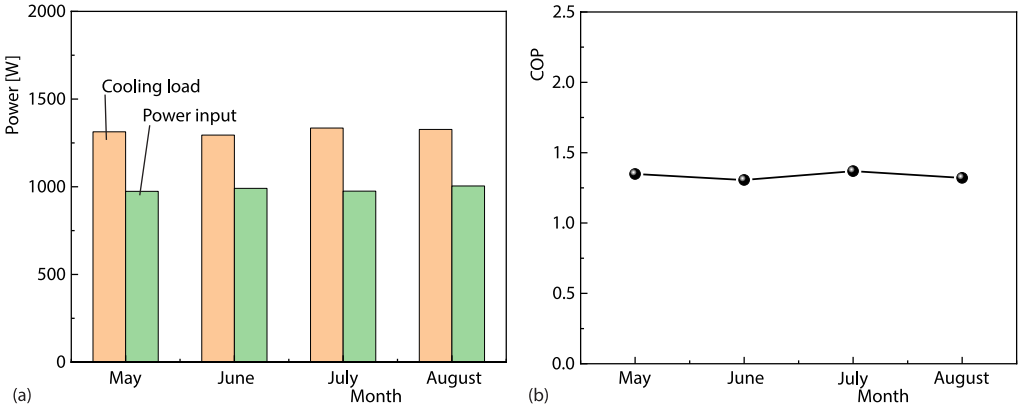

Figure 6. Monthly system performance of GS-PSRC

Moreover, it is clear that the outdoor wind speed negatively affects the cooling capacity of the system from the previous analysis leads to a lower monthly cooling capacity of the system, which is also a direct cause of the lower COP of the system. The contribution of different heat transfer mechanisms to the cooling capacity of the GS-PSRC system is analyzed in fig. 7, which shows the monthly cooling capacity (*i.e.*, heat dissipation) generated through the radiators, and the negative cooling generation means that the radiators are heated by the environment. It is found that although the radiators produce a large amount of cooling through radiative heat transfer during the period of May to August, the cooling effect is weakened by the high outdoor wind speeds that cause convective heat transfer to be almost dominant, as shown in fig. 7. In other words, although the GS-PSRC system can produce net cooling capacity in areas with high wind speeds, its cooling capacity has a limited and it may only be applied to buildings with low cooling demand or indirect cooling.

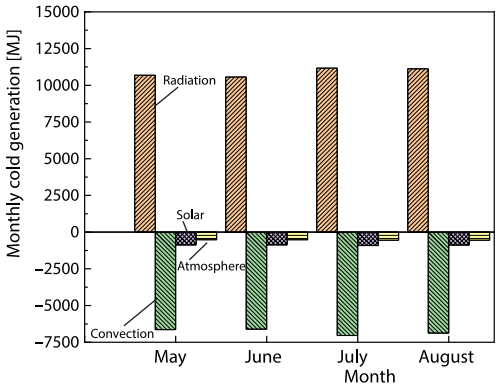

Figure 7. The contributions from radiative cooling, solar, atmosphere and convection, respectively

Overall, the GS-PSRC system is able to produce a certain amount of cooling capacity for the building and can maintain the temperature of the cold storage tank well below the ambient temperature at all times, as shown in fig. 5(d). Therefore, it can be seen that the GS-PSRC system is sufficient to satisfy the building's cooling needs, but when the building's demand for cooling is greater, it is recommended that windbreaks around the radiators be installed to mini-

mize the weakening of the cooling capacity due to convection. In addition, since convection is negative in the summer months, this may lead to more frequent operation of the system under sub-ambient conditions, which may increase electricity consumption.

The effect of climate zones on system performance

To show the climatic adaptability of the GS-PSRC system, more cases have been studied for the same building in different climatic regions, including Beijing (cold zone), Xi'an (cold zone), Nanchang (hot-summer and cold-winter zone), and Guangzhou (hot-summer and warm-winter zone). The parameters of the GS-PSRC system are different in different climatic conditions, and the surface area of the radiators and the volume of the cold storage tanks in each region can be calculated according to eqs. (10) and (11), as shown in tab. 5. Due to large cooling load requirement, the surface area of the radiators required in Nanchang area is slightly larger than the roof area (50 m^2), and the area beyond the roof can be extended out of the roof. The trend of the average monthly COP in summer for five different regions is shown in fig. 8. The average summer COP of Chengdu, Beijing, Xi'an, Nanchang, and Guangzhou are 1.34, 1.57, 1.47, 1.75, and 1.37, respectively, which shows that the average COP of the system do not differ much in different climatic zones. Although Xi'an and Beijing are located in the cold region, they can still perform well in summer, and thus it can be demonstrated that the system has good regional adaptability. Especially, the monthly average COP curve for Guangzhou shows that the high summer temperatures coupled with high outdoor wind speeds inhibit the ability of the GS-PSRC to generate low temperature cooling water, making the overall performance of the system slightly worse than in other climatic zones.

Table 5. Parameters of the sky radiative cooling system in different climate conditions

Location	Radiator surface area [m^2]	Volume of water tank [m^3]
Beijing	47.4	6.8
Xi'an	47.8	7.1
Nanchang	51.2	7.6
Guangzhou	46.6	6.9

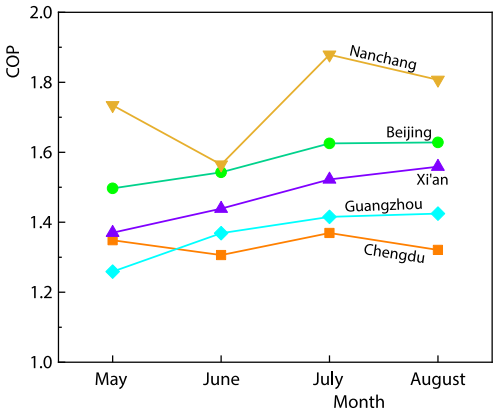

Figure 8. Climate adaptability of the GS-PSRC system of monthly averaged COP variation in five different climate conditions

Conclusion

A novel GS-PSRC system for building cooling is proposed. The sky radiative cooling subsystem can provide 24 hour continuous cooling through the use of a recently developed grating selective structure, which has an average infrared emissivity of greater than 88% and reflects more than 95% of solar radiation during the day [28]. The cold produced by the GS-PSRC system can be stored in a cold storage tank to supply cooling to the building according to different operation modes. Taking the Chengdu area as an example, a simulation analysis of a 50 m^2 office building during the hottest week of summer shows that the system can maintain an indoor temperature difference of 3.39-10.77 °C when the daily maximum ambient temperature is between 30.25 °C and 36.3 °C, with a monthly average COP of about 1.34 in summer. In addition, it was found that high outdoor wind speed would lead to almost dominant role of

convective heat transfer, which would inhibit the cooling capacity of the sky radiative cooling subsystem. Therefore, when using this system for cooling, it is recommended to add wind blocking devices around the radiant panels to weaken the effect of wind speed on the radiators. This study is a good demonstration of the potential of GS-PSRC system for application in building energy efficiency.

Acknowledgment

The funding source for this research is provided by the Sichuan Provincial Department of Housing and Urban-Rural Development Subject SCJSKJ2022-21.

Reference

[1] Goldstein, E. A., *et al*., Sub-Ambient Non-Evaporative Fluid Cooling with The Sky, *Nature Energy*, *2* (2017), 17143
[2] Liu, J., *et al*., Advances and Challenges in Commercializing Radiative Cooling, *Materials Today Physics*, *11* (2019), 100161
[3] Liu, J., *et al*., Recent Advances in the Development of Radiative Sky Cooling Inspired from Solar Thermal Harvesting, *NanoEnergy*, *81* (2020), 105611
[4] Shi, J., *et al*., Electrocaloric Cooling Materials and Devices for Zero-Global-Warming-Potential, High-Efficiency Refrigeration, *Joule*, *3* (2019), 5, pp. 1200-1225
[5] Singh, G. K., Solar Power Generation by PV (photovoltaic) Technology: A Review, *Energy*, *53* (2013), May, pp. 1-13
[6] Singh, V. K., Singal, S. K., Operation of Hydro Power Plants – A Review, *Renewable & Sustainable Energy Reviews*, *69* (2017), Mar., pp. 610-619
[7] Vargas, S. A., *et al*., Wind Power Generation: A Review and a Research Agenda, *Journal of Cleaner Production*, *218* (2019), May, pp. 850-870
[8] Raman, A. P., *et al*., Passive Radiative Cooling Below Ambient Air Temperature under Direct Sunlight, *Nature*, *515* (2014), 7528, pp. 540-544
[9] Hsu, P. C., *et al.*, Radiative Human Body Cooling by Nanoporous Polyethylene Textile, *Science*, *353* (2016), 6303, p. 1019-1023
[10] Zhai, Y., *et al*., Scalable-Manufactured Randomized Glass-Polymer Hybrid Metamaterial for Daytime Radiative Cooling, *Science*, *355* (2017), 6329, pp. 1062-1006
[11] Mandal, J., *et al*., Hierarchically Porous Polymer Coatings for Highly Efficient Passive Daytime Radiative Cooling, *Science*, *362* (2018), 6412, pp. 315-319
[12] Li, T., *et al*., A Radiative Cooling Structural Material, *Science*, *364* (2019), 6442, pp. 760-763
[13] Zeng, S., *et al*., Hierarchical-Morphology Metafabric for Scalable Passive Daytime Radiative Cooling, *Science*, *373* (2021), 6555, pp. 692-696
[14] Wang, S., *et al*., Scalable Thermochromic Smart Windows with Passive Radiative Cooling Regulation, *Science*, *374* (2021), 6574, pp. 1501-1504
[15] Pirvaram, A., *et al*., Radiative Cooling for Buildings: A Review of Techno-Enviro-Economics and Life-Cycle Assessment Methods, *Renewable and Sustainable Energy Reviews*, *162* (2022), 112415
[16] Zhang, J., *et al*., Cover Shields for sub-Ambient Radiative Cooling: A Literature Review, *Renewable and Sustainable Energy Reviews*, *143* (2021), 323, 110959
[17] Lin, K. T., *et al*., Radiative Cooling: Fundamental Physics, Atmospheric Influences, Materials and Structural Engineering, Applications and Beyond, *NanoEnergy*, *80* (2020), 105517
[18] Yu, X., *et al*., Review of Radiative Cooling Materials: Performance Evaluation and Design Approaches, *NanoEnergy*, *88* (2021), 106259
[19] Wu, Y., *et al*., A Review of the Application of Radiative Sky Cooling in Buildings: Challenges and Optimization, *Energy Conversion & Management*, *265* (2022), 115768
[20] Catalanotti, S., The Radiative Cooling of Selective Surfaces, *Sol. Energy*, *17* (1975), 2, pp. 83-89
[21] Sun, K., *et al*., VO2 Thermochromic Metamaterial-Based Smart Optical Solar Reflector, *ACS Photonics*, *5* (2018), 6, pp. 2280-2286
[22] Zhou, L., et al., Flexible Polymer Photonic Films With Embedded Microvoids For High-Performance Passive Daytime Radiative Cooling, *ACS Photonics*, *2021* (2021), 8, pp. 3301-3307
[23] Jaramillo-Fernandez, J., *et al*., Highly-Scattering Cellulose-Based LMS for Radiative Cooling, *Advanced Science, 9* (2022), 8, 2104758

[24] Zhang, Y., *et al*., Atmospheric Water Harvesting by Large-Scale Radiative Cooling Cellulose-Based Fabric, *Nanoletters*, *22* (2022), 7, pp. 2618-2626
[25] Herve, A., *et al*., Radiative Cooling by Tailoring Surfaces with Microstructures: Association of a Grating and a Multi-Layer Structure, *J. of Quantitative Spectroscopy and Rad. Transf*., *221* (2018), 1, pp. 155-163
[26] Dai, Y. D., *et al*., Radiative Cooling with Multilayered Periodic Grating under Sunlight, *Optics Communications*, *475* (2020), 15, 126231
[27] Zhang, Z., *et al*., Design of Selectively Multilayered Periodic Gratings by PSO Algorithm for Radiative Cooling, *Optics Communications*, *500* (2021), 127323
[28] Zhang, Z., *et al*., Passive Radiative Cooling Design with Novel Selectively Grating Structure under Direct Sunlight, *Optik*, *277* (2023), 170711
[29] Zhu, B., *et al*., Subambient Daytime Radiative Cooling Textile Based on Nanoprocessed Silk, *Nature Nanotechnology*, *16* (2021), 12, pp. 1342-1348
[30] Liu, Y., *et al.*, Acrylic Membrane Doped with Al_2O_3 Nanoparticle Resonators for Zero-Energy Consuming Radiative Cooling, *Solar Energy Materials and Solar Cells*, *213* (2020), 110561
[31] Yoon, T. Y., *et al*., Colloidal Deposition of Colored Daytime Radiative Cooling Films Using Nanoparticle-Based Inks, *Materials Today Physics*, *21* (2021), 100510
[32] Yin Baoquan, W. Y., *et al*., Performance Analysis of Multifunctional Building Energy System Based on Photovoltaic Radiation Panels, *Sichuan Building Science*, *1* (2014), 40, pp. 327-330
[33] Zhao, D., *et al.*, Roof-Integrated Radiative Air-Cooling System to Achieve Cooler Attic for Building Energy Saving, *Energy and Buildings*, *203* (2019), 109453
[34] Zhao, D., *et al*., Subambient Cooling of Water: Toward Real-World Applications of Daytime Radiative Cooling, *Joule*, *3* (2018), 1, pp. 111-123
[35] Aili, A., *et al*., A kW-Scale 24-hour Continuously Operational Radiative Sky Cooling System Experimental Demonstration and Predictive Modelling, *Energy Conversion and Management*, *186* (2019), pp. 586-596
[36] Zhou, K., *et al.*, Performance Analysis on System-Level Integration and Operation of Daytime Radiative Cooling Technology for Air-Conditioning in Buildings, *Energy and Buildings*, *235* (2021), 4, 110749
[37] Chen, L., *et al*., Sub-Ambient Radiative Cooling and Its Application in Buildings, *Building Simulation*, *13* (2020), 6, pp. 1165-1189
[38] Jeong, S. Y., *et al.*, A Numerical Study of Daytime Passive Radiative Coolers for Space Cooling in Buildings, *Building Simulation*, *11* (2018), 005, pp. 1011-1028
[39] Zhang, *et al*., Energy Saving and Economic Analysis of a New Hybrid Radiative Cooling System for Single-Family Houses in the USA, Applied Energy, *224* (2018), 815, pp. 371-381
[40] Wang, W., *et al*., Performance Assessment of a Photonic Radiative Cooling System for Office Buildings, *Renewable Energy*, *118* (2018), Apr., pp. 265-277
[41] Zhao, D., *et al.*, Radiative Sky Cooling-Assisted Thermoelectric Cooling System for Building Applications, *Energy, 190* (2020), 116322
[42] Liao, T., *et al*., Radiative Cooling-Assisted Thermoelectric Refrigeration and Power Systems: Coupling Properties and Parametric Optimization, *Energy*, *242* (2022), 122546
[43] Yin, X., *et al*., Terrestrial Radiative Cooling: Using the Cold Universe as a Renewable and Sustainable Energy Source, *Science*, *370* (2020), 6518, pp. 786-791
[44] Granqvist, G. C., Radiative Cooling to Low Temperatures: General Considerations and Application Selectively Emitting SiO Films, *Journal of Applied Physics*, *52* (1981), 6, pp. 4205-4220
[45] Shen, S. S., *et al*., MODTRAN5: 2006 Update, *Proceedings*, Algorithms and Technologies for Multispectral, Hyperspectral, and Ultraspectral Imagery XII, Orlando, Fla., USA, 2006, Vol. 6233
[46] Holman, J. P., *Heat Transfer*, McGraw-Hill, New York, USA, 6th ed., 2001
[47] Chae, D., *et al*., Spectrally Selective Inorganic-Based Multilayer Emitter for Daytime Radiative Cooling, *ACS Applied Materials & Interfaces*, *12* (2020), 7, pp. 8073-8081

Paper submitted: July 22, 2024
Paper revised: January 1, 2025
Paper accepted: January 10, 2025